

Molecular Dynamics Simulations of Layer-by-Layer Assembly of Polyelectrolytes at Charged Surfaces: Effects of Chain Degree of Polymerization and Fraction of Charged Monomers

Pritesh A. Patel,^{†,||} Junhwan Jeon,[‡] Patrick T. Mather,[‡] and
Andrey V. Dobrynin^{*,‡,§}

Department of Chemical Engineering, Polymer Program, Institute of Materials Science, and
Department of Physics, University of Connecticut, Storrs, Connecticut 06269, and
Macromolecular Science and Engineering, Case Western Reserve University,
Cleveland, Ohio 44106

Received February 17, 2005. In Final Form: April 14, 2005

We performed molecular dynamics simulations of the electrostatic assembly of multilayers of flexible polyelectrolytes at a charged surface. The multilayer build-up was achieved through sequential adsorption of oppositely charged polymers in a layer-by-layer fashion from dilute polyelectrolyte solutions. The steady-state multilayer growth proceeds through a charge reversal of the adsorbed polymeric film which leads to a linear increase in the polymer surface coverage after completion of the first few deposition steps. Moreover, substantial intermixing between chains adsorbed during different deposition steps is observed. This intermixing is consistent with the observed requirement for several deposition steps to transpire for completion of a single layer. However, despite chain intermixing, there are almost perfect periodic oscillations of the density difference between monomers belonging to positively and negatively charged macromolecules in the adsorbed film. Weakly charged chains show higher polymer surface coverage than strongly charged ones.

Introduction

Layer-by-Layer (LbL) assembly of charged molecules is a simple and versatile technique for the formation of nanolayered multicomponent films (see for review refs 1–9). These films are assembled by alternating exposure of a charge-bearing substrate to solutions of oppositely charged polyelectrolytes with a rinse step between to remove loosely adsorbed chains. Each exposure reverses the surface charge and thus reconstructs the surface properties, leaving it primed for the next adsorption of oppositely charged polyelectrolytes. Continued film growth is achieved by alternating the deposition of polyanions and polycations from their aqueous solutions and generally exhibits a linear increase in layer thickness (or mass) after

deposition of just a few layers. The simplicity of this technique with practically no limitations on the shape of the charge-bearing species allows the fabrication of multilayer films from synthetic polyelectrolytes, DNA,¹⁰ proteins,¹¹ nanoparticles,¹² etc. This has resulted in the utilization of multilayered films for sensors,¹³ light-emitting systems,¹⁴ selective area patterning,¹⁵ nonlinear optical devices and drug delivery,^{16a,b} as well as rapid processing via sequential spin-coating.¹⁷

Structural and physical properties of multilayered films assembled by the LbL technique have been studied extensively over the past 10 years. It has been established that: (i) multilayers are not stratified into well-defined layers but are interdiffused and intermixed,^{6,18} (ii) chain adsorption is irreversible on the time scale of multilayer assembly and the counterions do not participate in the charge balance within the multilayers,¹⁹ (iii) layer thick-

* Author to whom correspondence should be addressed. E-mail: avd@ims.uconn.edu.

† Department of Chemical Engineering, University of Connecticut.

‡ Case Western Reserve University.

|| Present address: Department of Chemical Engineering, Case Western Reserve University.

‡ Polymer Program, Institute of Materials Science, University of Connecticut.

§ Department of Physics, University of Connecticut.

(1) Iler, R. K. *J. Colloid Interface Sci.* **1966**, *21*, 569–594.

(2) Decher, G.; Hong, J. D. *Makromol. Chem., Macromol. Symp.* **1991**, *46*, 321–327.

(3) Decher, G.; Hong, J. D. *Ber. Bunsen-Ges. Phys. Chem.* **1991**, *95*, 1430–1434.

(4) Decher, G.; Schmitt, J. *Colloid Polym. Sci.* **1992**, *89*, 160.

(5) Decher, G. In *The Polymeric Materials Encyclopedia: Synthesis, Properties and Applications*; Slasmon, J. C., Ed.; CRC Press: Boca Raton, FL, 1996.

(6) Decher, G. *Science* **1997**, *277*, 1232–1237.

(7) Decher, G.; Eckle, M.; Schmitt, J.; Struth, B. *Curr. Opin. Colloid Interface Sci.* **1998**, *3*, 32–39.

(8) Hammond, P. T. *Curr. Opin. Colloid Interface Sci.* **1999**, *6*, 430–442.

(9) Decher, G.; Schlenoff, J. B., Eds. *Multilayer Thin Films-Sequential Assembly of Nanocomposite Materials*; Wiley-VCH: New York, 2003.

(10) Sukhorukov, G. B.; Mohwald, H.; Decher, G.; Lvov, Y. M. *Thin Solid Films* **1996**, 220–223.

(11) Rusling, J. F. In *Protein Architecture: Interfacing Molecular Assemblies and Immobilization Biotechnology*; Marcel Dekker: New York, 2000.

(12) Caruso, F.; Caruso, R. A.; Mohwald, H. *Science* **1998**, *282*, 1111–1113.

(13) Sun, Y.; Zhang, X.; Sun, C.; Wang, B.; Shen, J. *Macromol. Chem. Phys.* **1996**, *197*, 147–153.

(14) Fou, A. C.; Onitsuka, O.; Ferreira, M.; Rubner, M. F. *J. Appl. Phys.* **1996**, *79*, 7501–7509.

(15) Hammond, P. T.; Whitesides, G. M. *Macromolecules* **1995**, *28*, 7569–7571.

(16) (a) Laschewsky, A.; Mayer, B.; Wischerhoff, E.; Arys, X.; Bertrand, P.; Delcorte, A.; Jonas, A. *Thin Solid Films* **1996**, *284–285*, 334–337. (b) Burke, S. E.; Barrett, C. J. *Macromolecules* **2004**, *37*, 5375–5384.

(17) Lefaux, C. J.; Zimmerlin, J. A.; Dobrynin, A. V.; Mather, P. T. *J. Polym. Sci., Part B: Polym. Phys.* **2004**, *42*, 3654–3666.

(18) Decher, G.; Lvov, Y.; Schmitt, J. *Thin Solid Films* **1994**, *244*, 772–777.

(19) Schlenoff, J. B.; Ly, H.; Li, M. *J. Am. Chem. Soc.* **1998**, *120*, 7626–7634.

ness and molecular organization of adsorbed polymers can be precisely tuned by varying salt concentration, solvent quality, polyelectrolyte charge density, pH of the solutions, etc.;²⁰ (iv) polymer concentration, molecular weight, and deposition time are less influential parameters;^{4,6} and (v) oppositely charged monomers form ion pairs and the adsorption is limited by the electrostatic barrier at the surface.²¹ Despite the significant amount of work done on the experimental side of the problem, the theoretical understanding of the LbL process is still in its infancy.^{17,20,22–26} One of the main reasons for the slow development of theoretical models for LbL processes is the difficulty associated with experimental verification of the assumptions made in theoretical models. At this stage, molecular simulations offer a very valuable and useful tool that can help in understanding the physical mechanisms governing LbL assembly.

Monte Carlo simulations of a multilayered film assembly from mixtures of oppositely charged polyelectrolytes near charged spherical particles and a uniformly charged surface were performed by Messina et al.^{27–29} These papers tested the hypothesis that multilayering is an equilibrium process which occurs not only when one proceeds in a stepwise fashion, as done in experiments, but also when oppositely charged polyelectrolytes are added together and the resulting solution is exposed to a charged substrate. It was shown that the additional short-range attractive interactions between polyelectrolytes and the surface are required to successfully initiate film growth. Unfortunately, these simulations were limited to only a few deposition steps; thus, the system was far from reaching a stationary regime in which film thickness and mass increased linearly with the number of deposition steps as seen in experiments. This shortcoming was addressed in the recent molecular dynamics (MD) simulations by Panchagnula et al.^{30,31} that studied the sequential adsorption of oppositely charged polyelectrolytes onto a charged spherical particle. These simulations confirmed that layer build-up proceeds through surface overcharging during each deposition step and that the system reaches a steady-state regime after a few deposition steps with nonlinear growth of polymer mass in the aggregate. Despite this steady growth, however, the spherical symmetry of such a macro ion precluded formation of the well-developed multilayered structures.

In this paper, we present MD simulations of multilayer formation from dilute polyelectrolyte solutions at a charged planar surface with discrete charge distribution. The sequential deposition process implemented in our simulations resembles a real experimental situation in which there is alternating deposition of oppositely charged polyelectrolytes with removal of unadsorbed excess poly-

electrolyte by a rinse step. We present a detailed study of multilayer formation and layer structure including the effects of both fraction of charged monomers on polymer backbone and chain degree of polymerization on the polymer density distribution in a growing film; surface morphology, intermixing, and interdiffusion of polyelectrolyte chains between layers and ion pair formation between oppositely charged macromolecules.

Model and Simulation Method

The MD simulations of multilayer assembly are performed from dilute polyelectrolyte solutions of chains with degree of polymerizations $N_p = 32, 16,$ and 8 . The fraction of charged monomers on each chain is equal to $f = 1, 1/2,$ or $1/3$, corresponding to every, every second, and every third monomer carrying a charge. All the combinations of charge fraction, f , and the chain degree of polymerization, N_p , were studied except for the system with fraction of charged monomers $f = 1/3$ and degree of polymerization $N_p = 8$. The charge distribution for this system is asymmetric, resulting in a charge sequence effect. Polyelectrolytes are modeled as bead-spring chains consisting of N_p monomers of diameter σ . The connectivity of beads in the chains is maintained by the finite extensible nonlinear elastic (FENE) potential³²

$$U_{\text{FENE}}(r) = -0.5k_s R_{\text{max}}^2 \ln\left(1 - \frac{r^2}{R_{\text{max}}^2}\right) \quad (1)$$

with the spring constant $k_s = 30k_B T/\sigma^2$, where k_B is the Boltzmann constant and T is the absolute temperature, and the maximum bond length being $R_{\text{max}} = 1.5\sigma$. Counterions with diameter σ are explicitly included in our simulations to preserve the system electroneutrality. Electrostatic interaction between any two charged particles bearing charge valences q_i and q_j , and separated by a distance r_{ij} is given by the Coulomb potential:

$$U_{\text{Coul}}(r_{ij}) = k_B T \frac{l_B q_i q_j}{r_{ij}} \quad (2)$$

where l_B is the Bjerrum length, $l_B = e^2/\epsilon k_B T$, defined as the length scale at which the Coulomb interaction between two elementary charges, e , in a dielectric medium of dielectric constant, ϵ , is equal to the thermal energy, $k_B T$. For our simulations, the Bjerrum length was fixed at $l_B = 1.0\sigma$. All charged particles in our simulations are monovalent ions with valence $q_i = \pm 1$.

The adsorbing surface was modeled by a periodic hexagonal packed lattice of particles with diameter σ located at $z = 0$. Every second particle on the lower surface has univalent charge. A similar but uncharged nonselective surface was located in the opposite side of the simulation box to prevent chains from escaping and, hence, maintain 2-D periodicity in the lateral (x and y) directions. The system size is $20\sigma \times 20.784\sigma \times 80\sigma$ for systems with a fraction of charged monomers $f = 1$ and $1/2$. For the systems with $f = 1/3$, the box size is $20\sigma \times 20.784\sigma \times 160\sigma$ to have enough charges in a system to overcharge a surface at a monomer concentration of $0.038\sigma^{-3}$. The particle-particle particle-mesh (PPPM) method for the slab-geometry implemented in LAMMPS³³ with the sixth-order charge interpolation scheme was used to calculate the electrostatic interactions in the system. In this method, the 2-D periodic images of the system are periodically replicated along the z direction with distance $L = 3L_z$ between their boundaries. This reduces the problem of calculation of the electrostatic interactions in a 2-D periodic system to those in a 3D system.

In addition to electrostatic interactions, both charged and uncharged particles in the system interact through a truncated-shifted Lennard-Jones (LJ) potential.

(20) Dubas, S. T.; Schlenoff, J. B. *Macromolecules* **1999**, *32*, 8153–8160.

(21) Lowack, K.; Helm, C. A. *Macromolecules* **1998**, *31*, 823–833.

(22) Netz, R.; Joanny, J. F. *Macromolecules* **1999**, *32*, 9013–9025.

(23) Schlenoff, J. B.; Dubas, S. T. *Macromolecules* **2000**, *34*, 592–598.

(24) Castelnovo, M.; Joanny, J. F. *Langmuir* **2000**, *16*, 7524–7532.

(25) Solis, F. J.; Cruz, M. O. d. l. *J. Chem. Phys.* **1999**, *110*, 11517–11522.

(26) Park, S. Y.; Rubner, M. F.; Mayes, A. M. *Langmuir* **2002**, *18*, 9600–9604.

(27) Messina, R.; Holm, C.; Kremer, K. *Langmuir* **2003**, *19*, 4473–4482.

(28) Messina, R. *Macromolecules* **2004**, *37*, 621–629.

(29) Messina, R.; Holm, C.; Kremer, K. *J. Polym. Sci., Part B: Polym. Phys.* **2004**, *42*, 3557–3570.

(30) Panchagnula, V.; Jeon, J.; Dobrynin, A. V. *Phys. Rev. Lett.* **2004**, *93*, 037801.

(31) Panchagnula, V.; Jeon, J.; Rusling, J. F.; Dobrynin, A. V. *Langmuir* **2004**, *21*, 1118–1125.

(32) Binder, K., Ed. *Monte Carlo and Molecular Dynamics Simulations in Polymer Science*; Oxford University Press: New York, 1995.

(33) Plimpton, S. J. *Comput. Phys.* **1995**, *117*, 1–19.

$$U_{LJ}(r) = \begin{cases} 4\epsilon_{LJ} \left[\left(\frac{\sigma}{r} \right)^{12} - \left(\frac{\sigma}{r} \right)^6 - \left(\frac{\sigma}{r_{\text{cut}}} \right)^{12} + \left(\frac{\sigma}{r_{\text{cut}}} \right)^6 \right] & \text{for } r \leq r_{\text{cut}} \\ 0 & \text{for } r > r_{\text{cut}} \end{cases} \quad (3)$$

A cutoff distance of $r_{\text{cut}} = 2.5\sigma$ is chosen for the surface particles/polymer–polymer interaction while a smaller value, $r_{\text{cut}} = 2^{1/6}\sigma$, was selected for polymer–counterion, surface particle–counterion, and counterion–counterion interactions. The interaction parameter was equal to $\epsilon_{LJ} = k_B T$ for all pairwise interactions. However, despite of relatively strong short-range interactions, none of the polymers studied are in the collapsed globular state. The complete polymer collapse is precluded by the electrostatic repulsion between charged monomers.

As we are interested in general class of polyelectrolyte multilayer formation, each bead in the coarse-grained bead–spring model used in our simulations represents several chemical units. If we assume that our Bjerrum length, $l_B = 1\sigma$, is equal to the Bjerrum length in aqueous solutions at room temperature ($T = 298\text{ K}$), $l_B = 7.14\text{ \AA}$, the monomer size is equal to $\sigma = 7.14\text{ \AA}$. This corresponds to approximately 2.9 monomers of NaPSS with monomer size 2.5 \AA . This leads to a chain degree of polymerization for $N_p = 32$ to be of the order of 100 monomers.

During each deposition step, the simulations are carried out in a constant number of particles, volume, and temperature (NVT) ensemble. The constant temperature is maintained by coupling the system to a Langevin thermostat. In this case, the equation of motion for the i^{th} particle is

$$m \frac{d\vec{v}_i}{dt}(t) = \vec{F}_i(t) - \xi \vec{v}_i(t) + \vec{F}_i^R(t) \quad (4)$$

where \vec{v}_i is the bead velocity, and \vec{F}_i is the net deterministic force acting on the i^{th} bead of mass m . \vec{F}_i^R is the stochastic force with zero average value and δ -functional correlations $\langle \vec{F}_i^R(t) \vec{F}_i^R(t') \rangle = 6\xi k_B T \delta(t - t')$. The friction coefficient was set to $\xi = m/\tau_{LJ} = 1/\tau_{LJ}$, where τ_{LJ} is the standard LJ time, $\tau_{LJ} = \sigma(m/\epsilon_{LJ})^{1/2}$, and m is a particle mass that was set to 1. The velocity–Verlet algorithm with a time step $\Delta t = 0.01\tau_{LJ}$ was used to integrate the equations of motion (eq 4).

Simulations were performed using the following procedure. Counterions from the charged surface were uniformly distributed over the simulation box. Then, M_1 negatively charged polyelectrolytes with N_p monomers corresponding to monomer concentration of $0.038\sigma^{-3}$ (e.g., $M_1 = 40$ for $N_p = 32$ and $f = 1/2$), together with their counterions, were added to the simulation box and simulations continued until completion of the first deposition step. For chains with fraction of charged monomers $f = 1/3$, the number of chains with degree of polymerization $N_p = 32$ was $M_1 = 80$ to maintain the same concentration of polyelectrolytes since the simulation box size was doubled in the z direction. After completion of the first simulation run (‘dipping’ step), unadsorbed polyelectrolyte chains were removed (‘rinsing’ step). Between steps, we separate the unadsorbed polyelectrolytes from adsorbed ones using a cluster algorithm³⁴ with a cutoff radius equal to 1.2σ . Additionally, between adsorption steps, the only counterions required to maintain the system electroneutrality (compensating for the excess charge in the growing polymeric layer) were kept in the simulation box. At the beginning of the second step, the simulation box is refilled with $M_2 = M_1$ oppositely charged polyelectrolytes together with their counterions. The concentration of newly added polyelectrolytes is the same as before, $0.038\sigma^{-3}$. This, then, is followed by another simulation run. We repeated these dipping and rinsing steps 12 times.

It is important to optimize the number of integration steps for each simulation run (deposition step) required for the system to reach saturation of the polymer-adsorbed amount and to approach equilibrium or the steady-state regime. The increase in the amount of adsorbed polymers in the growing layers was monitored

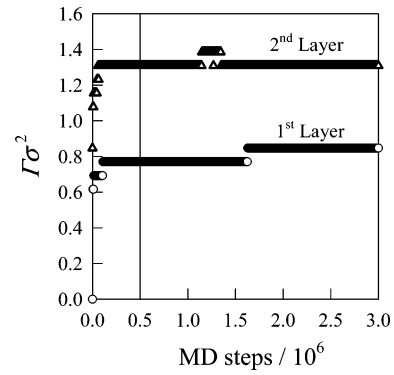


Figure 1. Dependence of the polymer surface coverage ($\Gamma\sigma^2$) on the number of MD integration steps for system with $N_p = 32$ and $f = 1$ during the first and the second deposition step for duration of 3.0×10^6 integration steps in each deposition step.

by plotting the polymer surface coverage, Γ , defined as the total number of adsorbed monomers normalized by the surface area of the charged planar surface, S , as a function of the number of integration (MD) steps. Figure 1 shows the evolution of the polymer surface coverage for the first two deposition steps for fully charged polyelectrolytes with $f = 1$ of degree of polymerization $N_p = 32$ during the simulation runs with a duration of 3×10^6 integration steps. For both cases there is relatively fast saturation in the adsorption amount (about 90%) during the first 5×10^4 integration steps. Hence, the duration of the simulation run for each deposition step were set to 5×10^5 integration steps, which is about 10 times longer than is necessary to achieve a saturation limit. However, as we have already mentioned, the simulation box was doubled in size for simulations of weakly charged polyelectrolyte chains with $f = 1/3$ and $N_p = 32$ and 16 by keeping the same concentration. In this case, the duration of each simulation run was increased up to 1.5×10^6 integration steps to allow polymer chains to diffuse through the enlarged simulation box. Our simulation corresponds to Rouse dynamics of a polymer chain for which the chain’s relaxation time increases with the chain degree of polymerization N_p as N_p^2 . Thus, the selected length of simulation runs is also sufficient for shorter polyelectrolyte chains with degree of polymerization $N_p = 16$ and 8 to reach the steady-state regime.

Results

Formation of Multilayers. Figure 2 shows the evolution of the layer build-up during the first five deposition steps for fully charged chains, $f = 1$, of the degree of polymerization $N_p = 32$. After the first deposition step, the polyelectrolyte chains almost uniformly cover the whole adsorbing surface. The few loops and tails that are formed contribute to the overcharging and the surface charge reversal necessary for reconstruction of surface properties and continuation of the chain adsorption during the next deposition step. Interestingly, after completion of the second deposition step, the adsorbed chains do not completely cover the substrate but instead leave islands with high polymer content coexisting with empty regions protruding down to the bare surface. These islands are less pronounced for partially charged chains ($f = 1/2$) compared to the fully charged chains ($f = 1$). During the third deposition step, adsorbing polyelectrolyte chains bear the same charge as those being adsorbed during the first deposition step. Thus, these chains adsorb onto the islands formed by oppositely charged polyelectrolyte chains from the second deposition step and refill the empty spots on the surface (see third step in Figure 2). The polyelectrolytes added into the simulation box during the fourth deposition cycle have the same charge as those adsorbed during the second deposition step. These chains refill the empty spots being left after completion of the third deposition step and then start formation of the fourth layer on top of the

(34) A chain is considered to belong to a cluster if it has at least one monomer within distance 1.2σ from any monomer belonging to a chain forming the cluster. The cluster analysis was performed by analyzing the matrix of distances between all monomers in the system.

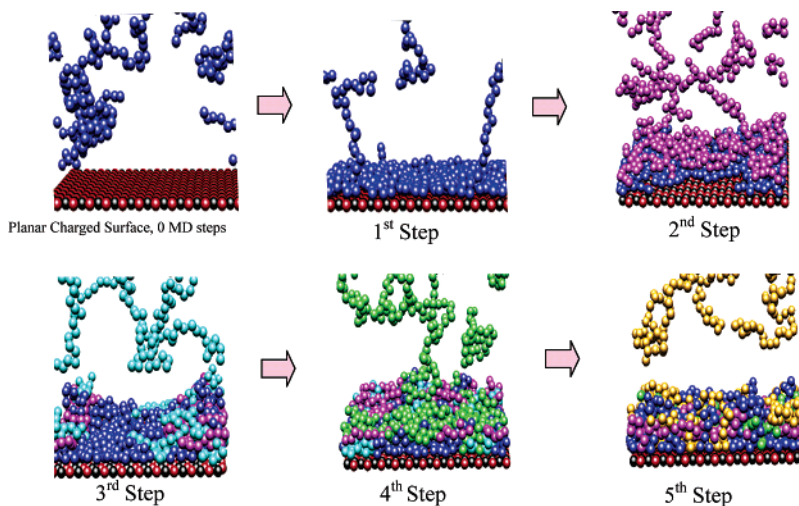


Figure 2. Evolution of the layer structure during the adsorption of fully charged ($f = 1$) polyelectrolytes, with degree of polymerization $N_p = 32$. Each snapshot is taken after the completion of deposition cycles from 1 through 5 with unique color coding for each step being maintained from one snapshot to the next. For example, the blue chain in the fifth step snapshot is polymer adsorbed originally during the first step. Counterions are not shown.

oppositely charged polymers deposited during the third deposition step. Further layer growth proceeds in similar fashion such that two deposition steps of similarly charged polymers are usually required for the completion of a single layer. The described pattern of the layer formation was seen for all 12 deposition steps performed in each simulated system. The polymer surface coverage, Γ , and average thickness of the adsorbed layers increase linearly with each deposition step for all the systems studied (see Figure 5 below). A steady-state linear growth regime is generally observed in experiments once the first few layers have been deposited.²³

A density profile of positively and negatively charged monomers in the multilayers after completion of the third deposition step is shown in Figure 3a. The monomer density of negatively charged chains, $\rho_-(z)$, shows two peaks near 1σ and 3σ that correspond to the first and third deposition steps of negatively charged polyelectrolytes. The only peak in the density profile of positively charged chains, $\rho_+(z)$, corresponds to monomers adsorbed during the second deposition step. The first peak near the surface has higher amplitude as compared to the peaks corresponding to the chains adsorbed during the second and third deposition steps. This is due to the high surface charge density in comparison with the value of the surface overcharging achieved after completion of the each deposition step. The large amount of polyelectrolytes adsorbed during the first deposition step is required to compensate for the surface charge, as well as to overcharge the surface for subsequent layer build-up. The strong surface charge effect is reminiscent of the one observed in experiments where the initial growth rate of the film is different than the growth rate observed in a steady-state regime. Experiments have shown that the surface charge could influence the layer build-up for as many as the first six deposition steps.³⁵ Figure 3b shows the density profile after completion of four deposition steps. Since polyelectrolytes deposited during the fourth deposition step have the same charge as those adsorbed during the second deposition step, the monomer density, $\rho_+(z)$, of positively charged chains increases. However, the majority of newly adsorbed monomers are added at a distance of about 2σ , corresponding to formation of the second layer

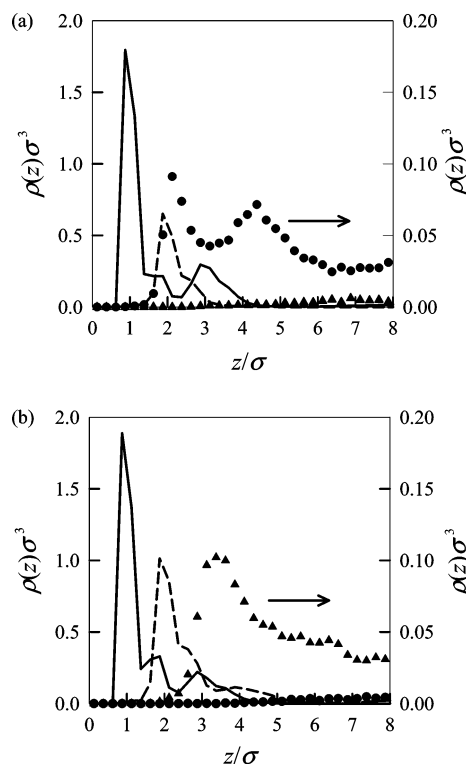


Figure 3. Density profiles of the negatively $\rho_-(z)$ (continuous line) and positively $\rho_+(z)$ (dashed line) charged monomers for system with fully charged ($f = 1$) polyelectrolyte chains with $N_p = 32$ after completion of (a) third and (b) fourth deposition steps with a duration of 5×10^5 MD steps each. The density profile of positively (circles) and negatively (triangles) charged counterions are also shown in the secondary axis.

of positively charged chains with a small amount of monomer being added on the top of the third (negatively) charged layer. Interestingly, the third layer peak observed in Figure 3a disappears after the fourth deposition step, giving rise to a slight increase in polymer density near the surface. This could be explained by the filling of the holes that were formed on the surface after the second and third deposition steps as shown in Figure 2.

To evaluate the surface topography, the monomer height sorting algorithm was used to select a monomer located at the furthest distance away from the surface covered by

(35) Lvov, Y.; Ariga, K.; Onda, M.; Ichinose, I.; Kunitake, T. *Colloids Surf., A* **1999**, *146*, 337–346.

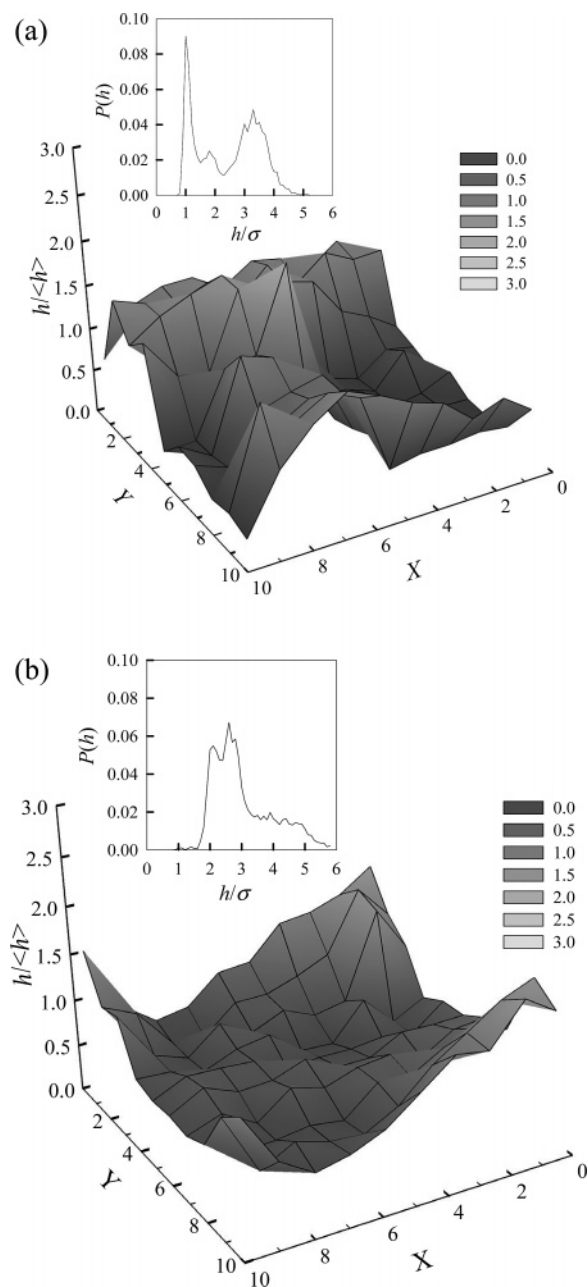


Figure 4. Topography plots of the film height distribution for the system of fully charged chains with $f = 1$ and degree of polymerization $N_p = 32$ at the end of 5×10^5 MD steps after the completion of third (a) and fourth (b) deposition steps. The inset shows the height distribution of the main plots.

(10×10) bins of size 2σ in the xy plane. The two-dimensional plot of this 10×10 matrix gives a surface topography that is analogous to atomic force microscopy (AFM) measurements. The average thickness of the layers was calculated as the average value of the height distribution. The standard deviation of this distribution was averaged after equilibration to obtain the average value of the surface roughness at each deposition step. Figure 4a and b shows the topography plots collected after the third and the fourth deposition steps. There are significant troughs present, indicating holes formed after the third deposition step. These holes are filled by newly incoming chains during the fourth deposition step. The multilayers rearrange and form a smooth surface after the fourth deposition step is completed. The surface roughness after completion of the third and fourth

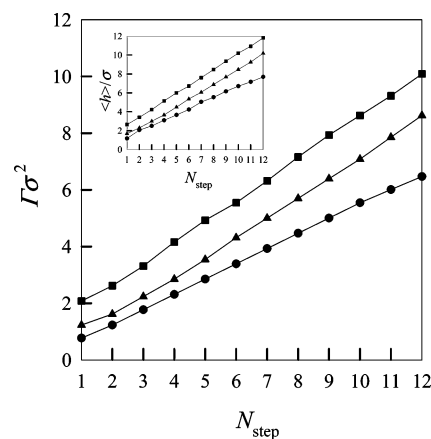


Figure 5. Dependence of the surface coverage ($\Gamma\sigma^2$) on the number of deposition steps for polyelectrolyte chains of the degree of polymerization $N_p = 32$ with different fraction of charged monomers $f = 1$ (circles), $1/2$ (triangles), and $1/3$ (squares). The inset show the dependence of average thickness on number of deposition steps.

deposition steps was equal to 1.125σ and 0.974σ , respectively. The insets in Figure 4a and b show the film height distribution function after the third and the fourth deposition steps. The presence of holes in these plots is manifested by the bimodal distribution, as it is seen in Figure 4a. In Figure 4b, the holes are filled during the subsequent deposition step, as suggested by the single peak distribution function indicating a relatively smooth surface.

Effect of Charge Density of Polyelectrolytes. The dependence of polymer surface coverage, Γ , on the fraction of charged monomers on the polymer backbone at different deposition steps is shown in Figure 5. As it follows, from this figure, the steady state regime is reached after completion of just the first few deposition steps for all polyelectrolyte systems with different charge fractions. This is indicated by the linear growth of the polymer surface coverage on the number of deposition steps. The average thickness of the adsorbed layer also increases linearly with the number of deposition steps for all studied systems (see inset in Figure 5). These linear dependences are observed despite the fact that two deposition steps are usually required to complete one layer. For partially charged chains with $f = 1/2$, the growth rate of polymer surface coverage is higher than for the case of fully charged chains. This is also in agreement with experimental observations of thicker layers for partially charged polyelectrolytes compared to very thin layers obtained for the fully charged polyelectrolytes, for which charge regulation was achieved by varying solution pH.¹⁹ In the case of partially charged chains, for each adsorbed charge, there are extra $1/f - 1$ monomers added to the adsorbed layer, thus allowing a larger number of monomer segments to be adsorbed per charged group in the underlying layer. For weakly charged chains with $f = 1/3$, however, although the surface coverage is higher than for fully charged chains, $f = 1$, and half charged ones, $f = 1/2$, the growth rate given by the slope is almost the same as that observed for systems with $f = 1/2$. The higher initial value of the surface coverage for adsorption of polyelectrolyte chains with $f = 1/3$ is due to surface effects where more chains are needed for surface charge compensation and overcharging. After deposition of the first two layers, the growth rate for the systems with $f = 1/3$ is similar to those observed for polyelectrolytes with $f = 1/2$.

The distribution of polymer density $\rho(z)$ during different deposition steps for chains with degree of polymerization

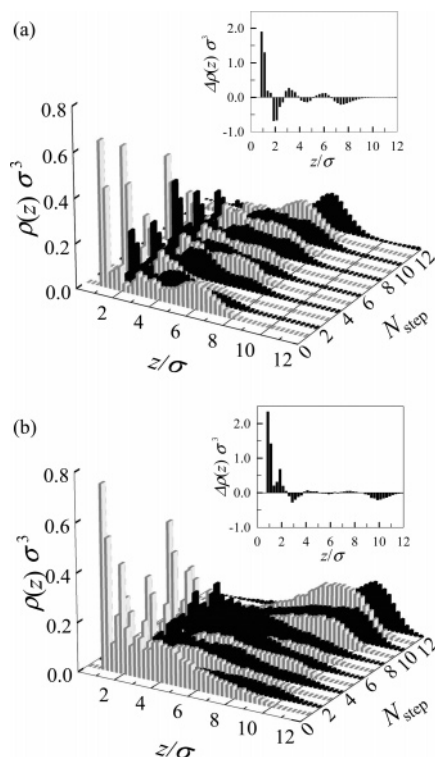


Figure 6. Density profiles of the fully charged ($f = 1$) (a) and partially charged ($f = 1/2$) (b) polyelectrolyte chains with $N_p = 32$ after completion of 12 deposition cycles with duration of 5×10^5 MD steps each. Insets show the difference between the corresponding uniaxial monomer densities of positively and negatively charged chains, $\Delta\rho(z) = \rho_-(z) - \rho_+(z)$.

$N_p = 32$ and fraction of charged monomers $f = 1$ and $1/2$ are shown in Figure 6a and b. These distribution functions were averaged separately for each set of adsorbed chains during different deposition steps for the duration of time required for deposition of the final layer. This procedure allows clear inspection of the interpenetration of the layers during the deposition process. There is a significant intermixing between polyelectrolyte chains adsorbed during different deposition cycles, though less so for the outermost layer. Despite such intermixing, a multilayered nature of the adsorbed polymeric film persists. This can be seen in the Figure 6a inset, which shows the difference between local monomer density of positively and negatively charged species. This plot clearly indicates the existence of alternating layers with excesses of positively or negatively charged polymeric components. The interpenetration between layers is enhanced for partially charged chains with fraction of charged monomers $f = 1/2$, as shown in Figure 6b. Close inspection of this distribution function reveals the presence of a broader polymer density distribution with lower magnitude.

The dependence of the density distribution function on the duration of the simulation run could potentially reveal whether the observed oscillations are kinetically trapped states or are representative of an equilibrium state. Figure 7 compares the density difference between positively and negatively charged chains for short (5×10^5 MD steps) and long simulation runs (3×10^6 MD steps) for the 12th deposition step. The density difference profile or the net charge distribution among the layers is remarkably close for both simulations, suggesting that multilayers are an equilibrium state. Interestingly, analysis of the density distribution, $\rho(z)$, after long simulation runs shows a difference in the density profiles of the individual layers. In particular, the sharp peak of the 12th deposition step

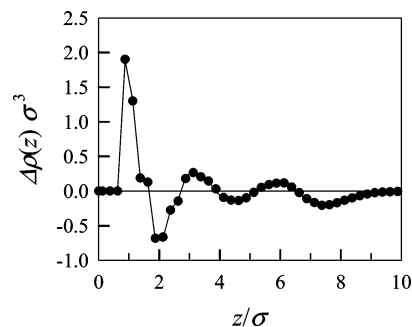


Figure 7. Comparison of the density difference of positively and negatively charged monomers, $\Delta\rho(z) = \rho_-(z) - \rho_+(z)$ for two different lengths of simulation runs. (i) 5×10^5 (circles) and (ii) 3×10^6 MD steps (continuous line).

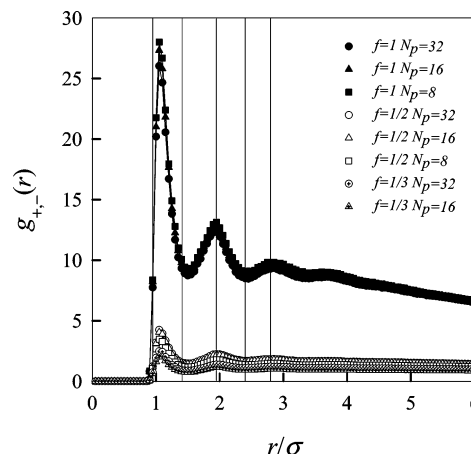


Figure 8. Ion pair correlation functions for chains with different fractions of charged monomers and different degrees of polymerization. The vertical reference lines show the peak positions of the perfectly stratified molecular layers of positively and negatively charged ions.

(outermost layer) seen in Figure 6a disappears for longer simulation run. The polyelectrolytes adsorbed during this deposition step diffuse further into the multilayers by keeping the density variations among the layers intact. This suggests that a dynamic exchange of the polyelectrolytes within the layers occurs by preserving the density difference between positively and negatively charged monomers among the layers. The intermixing between layers also indicates that the polymers at the surface are in the liquid state.

The formation of ionic pairs between oppositely charged groups in the multilayers is characterized by the charge–charge correlation function $g_{+,-}(r)^{37}$ between positively and negatively charged monomers. This function gives the probability of finding a negatively charged monomer at a distance r from a selected positively charged one. Figure 8 shows the charge–charge correlation function for all studied systems averaged after equilibration. All correlation functions have a maximum at a distance slightly greater than 1σ . This is approximately equal to the distance of the closest approach between monomers forming an ionic pair. The other distances at which such ionic correlations are enhanced—where these correlation functions show secondary and tertiary peaks—are equal to 1.95σ and 2.8σ . Vertical reference lines show the peak positions of the charge–charge correlation function for completely stratified molecular layers of polyelectrolyte

(36) Glinel, K.; Moussa, A.; Jonas, A. M.; Laschewsky, A. *Langmuir* **2002**, *18*, 1408–1412.

(37) Rapaport, D. C. Cambridge University Press: New York, 1995.

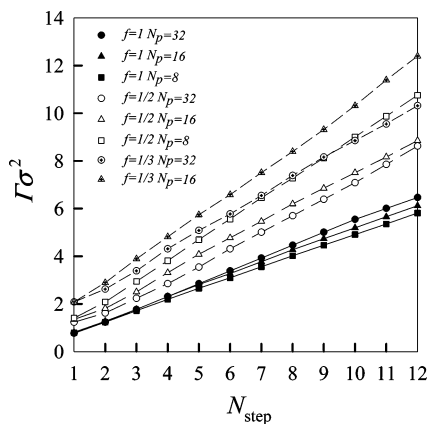


Figure 9. Dependence of the surface coverage ($\Gamma\sigma^2$) on the number of deposition steps for polyelectrolyte chains with different fraction of charged monomers and chain degree of polymerization.

chains covering the whole surface. The oppositely charged polyelectrolyte layers in this stratified film are shifted by a distance of $\sigma/2$ with respect to one another along the x direction. At least for the first three, these reference peaks are very close to the observed peaks, indicating some structured layering of ion pairs. Although these peak positions are the same for all our systems, their magnitudes decrease with decreasing fraction of charged monomers on the polymer backbone. Another important feature seen in Figure 8 is the effect of the chain's degree of polymerization, N_p , on ion pair distribution. For fully charged chains ($f = 1$), there is no effect of chain degree of polymerization on the shape of the charge–charge correlation function. However, for partially charged chains with fraction of charged monomers $f = 1/2$, the charge–charge correlation function shows weak dependence on the chain degree of polymerization. Figure 8 also gives important information on the relative density of ion pairs for multilayers formed by chains with different fractions of charged monomers. Thus, ion pairs could dictate the formation, stability, interpenetration, and chain dynamics observed in the multilayers.

Effect of Chain Degree of Polymerization. The dependence of the polymer surface coverage, Γ , during the film growth on the chain degree of polymerization is shown in Figure 9. For fully charged chains, $f = 1$, the growth rate increases slightly with the chain length, while partially charged chains yield a weak decrease in growth rate with increasing chain length. This N_p dependence can be explained by a combined effect of the discreteness of the net charge that each adsorbed chain delivers to the surface and the finite size effect of the simulation box. Each adsorbed chain delivers a quantized amount of charge not necessarily optimal for surface overcharging. Shorter chains allow better charge adjustment for the finite systems than the longer ones. This effect is even more pronounced for partially charged chains because, for each extra charged group, there are $1/f - 1$ uncharged ones added to the layer, leading to a larger difference in polymer surface coverage after each deposition step (see Figure 9). This is illustrated by the large difference in polymer surface coverage for weakly charged chains of monomer fraction $f = 1/3$ and degrees of polymerizations $N_p = 32$ and 16.

The chain degree of polymerization seems to have almost no effect on polymer density oscillations. Figure 10 shows the plot of the density difference between positively and negatively charged monomers for chain degree of polymerization $N_p = 8$ and different charge fractions of mono-

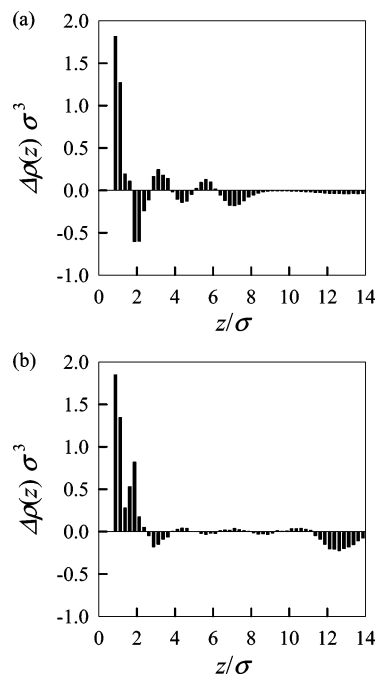


Figure 10. Comparison of density difference of positively and negatively charged monomers, $\Delta\rho(z) = \rho_-(z) - \rho_+(z)$ for chains degree of polymerization $N_p = 8$ and different fraction of charge monomers ($f = 1$ (a) and $1/2$ (b)).

mers ($f = 1$ and $1/2$). This remarkable similarity between the density oscillations for chains with different degrees of polymerization and the same charge fraction of monomers can be seen by comparing Figure 10 with Figure 6a and b insets. These density oscillations are also similar for chains with degree of polymerization $N_p = 16$ (not shown). This suggests that the chain degree of polymerization has almost no effect on polymer density oscillations. Shorter chains have high diffusivity between layers as compared with that for longer chains due to the lower amount of ion pairs per chain. This high mobility inside multilayers formed by shorter chains still preserves the layered structure and the symmetric oscillations observed for the systems of longer chains. This is similar to the results obtained for longer simulation runs using chains having degree of polymerization $N_p = 32$ as previously described in the discussion regarding Figure 7. The statement that longer simulation runs allowing further chain interdiffusion does not alter the periodic oscillation of the density difference observed within multilayers, thereby suggesting an equilibrated structure is thus reinforced.

Short chains with degree of polymerization $N_p = 8$ show dynamic exchange during the deposition process between adsorbed polyelectrolytes and those in solution. The frequency of chain exchange increases as the fraction of charged monomers on the polymer backbone decreases. This is another indication of the effect ion pairs have on chain dynamics. There are more ion pairs formed between oppositely charged chains inside multilayered films composed of strongly charged chains than in those of weakly charged ones. This leads to a higher energy barrier for adsorbed chains to overcome in order to escape from the adsorbed layer. This is supported by the fact that there is practically no exchange on the time scale of our simulation runs for fully charged chains with degree of polymerization $N_p = 32$. The number of exchanged chains, however, grows to about 10% of the total number of adsorbed chains during the whole deposition process, even for shorter chains with degree of polymerization $N_p = 8$.

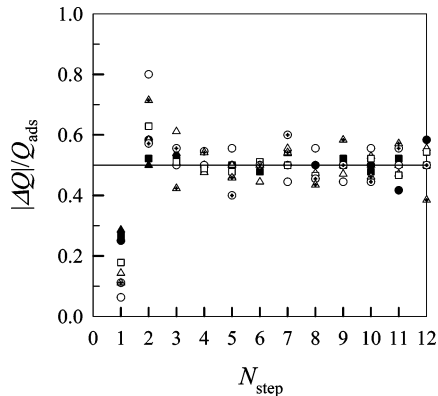


Figure 11. Dependence of overcharging fraction ($|\Delta Q|/Q_{\text{ads}}$) on the number of deposition steps for chains with different fractions of charged monomers and different degrees of polymerization. The symbols are the same as in Figure 9.

Schlenoff et al.¹⁹ have reported a slow exchange of the adsorbed polyelectrolyte chains along with a kinetically reversible nature of the deposited layers. In addition to this observation, we find that the probability of chain exchange decreases with increasing fraction of charged monomers on the polymer backbone, as well as chain degree of polymerization. It is worthwhile to note that, roughly, for each chain desorbed during the deposition step, an extra chain of the same type is simultaneously added, keeping the net value of layer overcharging nearly constant. This suggests that there is a simple relation between the overcharging and the number of charges adsorbed during each deposition step universal to all studied systems.

Universality. The universality of the overcharging process during steady-state film growth is shown in Figure 11. The ratio of the absolute value of the layer overcharging, $|\Delta Q|$, to the net charge carried by adsorbed chains at a given deposition step, $Q_{\text{ads}} = fN(s) - N(s-1)$ (where $N(s)$ is the total number of adsorbed monomers after completion of the s th step), is plotted versus the number of deposition steps N_{step} . This quantity appears to be relatively independent of the fraction of charged monomers on the polymer backbone, as well as the chain degree of polymerization. After several deposition cycles, when the system reaches a steady state, this ratio saturates at a value close to 1/2 for all studied systems. There is a very simple explanation for this phenomenon. For steady-state growth, one charge is needed per each excess ionic group to compensate for the surface charge while another is needed to recreate the surface properties for the adsorption of the next layer. If this ratio is smaller than 1/2, the film eventually stops growing; if it is more than 1/2, layer mass will show exponential growth. In both cases, the growth process is unstable. Fluctuations around this saturation value can be attributed to corresponding fluctuations in the number of adsorbed chains and should decrease with increasing system size. It is important to point out that the surface overcharging plays a two-fold role. First, it recreates the surface properties for the next deposition layer, and second, it prevents the unrestricted growth of the adsorbed amount which is stabilized by the electrostatic interactions between excess charges.

Theoretical Model of Multilayer Formation. The distribution of polymeric species inside the multilayered film (see Figures 6 inset, 7, and 10) resembles the layered structure assumed by Castelnovo et al.²⁴ However, this model does not account for the strong effect of short-range interactions and exclusion of counterions from the interior of the multilayered film established in our simulations.

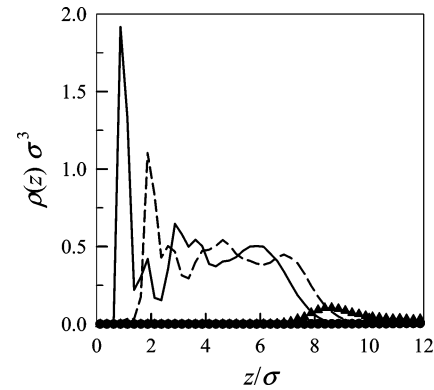


Figure 12. Density profiles of the negatively $\rho_{-}(z)$ (continuous line) and positively $\rho_{+}(z)$ (dashed line) charged monomers for system of fully charged ($f = 1$) polyelectrolyte chains with $N_p = 32$ after completion of twelfth deposition step with a duration of 5×10^5 MD steps each. The density profile of positively (circles) and negatively (triangles) charged counterions are also shown.

In light of the results described herein, the Castelnovo et al. model²⁴ can be modified to describe the polymer density profile and surface overcharging in the growing film (see Figure 12). In the concentrated mixture of positively and negatively charged chains, the oscillations of polymer density, $\Delta\rho$, with the period, d , is a result of the competition between two opposing effects: polymeric and electrostatic. The excess of the polymeric part of the system free energy per period, d , due to the one-dimensional density wave along the z direction of magnitude $\Delta\rho$ with respect to the average polymer density ρ is estimated as³⁸

$$\Delta F_{\text{pol}} \approx k_B T S \int_0^d \frac{\sigma^2}{\rho(z)} \left(\frac{d\rho(z)}{dz} \right)^2 dz \approx k_B T S \frac{\sigma^2 \Delta\rho^2}{\rho d} \quad (5)$$

This polymer density wave induces charge density oscillations of smaller magnitude ($f\Delta\rho$). The one-dimensional charge density wave formed in a multilayered film can be viewed as a system of parallel plate capacitors whose plates carry charge $Q_{\pm} \approx \pm ef\Delta\rho Sd$, are of area S , and are separated by a distance d . The electrostatic energy of such a parallel plate capacitor is

$$U_{\text{elect}} \approx k_B T S l_B (f\Delta\rho)^2 d^3 \quad (6)$$

(This estimate is only true in our case since the counterions are excluded from the adsorbed layer.) Thus, the optimal length scale of the density oscillation is obtained by minimizing polymeric and electrostatic contributions with respect to the period of oscillations, d . This leads to

$$d \approx (\sigma^2 / \rho l_B f^2)^{1/4} \quad (7)$$

The period of density oscillations increases with decreasing fraction of charged monomers on the polymer backbone as $f^{-1/2}$.²⁵ This inverse square-root dependence of the period of density oscillations is in agreement with the 1.32-fold increase of the parameter d seen in our simulations for systems with $f = 1/2$ (in comparison with that for systems of fully charged chains).

In the steady-state regime, the magnitude of the density oscillations is controlled by the layer overcharging. During each deposition step, the film overcharging, $|\Delta Q| \approx ef\Delta\rho d S$, is obtained by balancing the energy of electrostatic repulsion between unbalanced charges with the cohesive

(38) Grosberg, A. Y.; Khokhlov, A. R. *Statistical Physics of Macromolecules*; AIP Press: Melville, NY, 1994.

energy per monomer in a film, $k_B T \epsilon_{\text{coh}}$, and the interaction energy per monomer in a solution, $k_B T \epsilon_{\text{sol}}$. (These parameters, ϵ_{coh} and ϵ_{sol} , will be considered as adjustable parameters in the model.) The energy of electrostatic repulsion per excess charged monomer within a layer of excess charge, $|\Delta Q|$, exposed to a solution with the Debye radius, r_D , is estimated as

$$U_{\text{rep}} \approx k_B T \frac{l_B f \Delta \rho d r_D^2}{r_D} \approx k_B T l_B f \Delta \rho d r_D \quad (8)$$

The surface overcharging stops to grow when the energy of a chain with N_p monomers inside the overcharged region $N_p f U_{\text{rep}} - k_B T N_p \epsilon_{\text{coh}}$ is on the order of the chain's energy in a solution, $k_B T N_p \epsilon_{\text{sol}}$. Thus, the magnitude of the polymer density oscillations is estimated to be

$$\Delta \rho \approx (\epsilon_{\text{coh}} + \epsilon_{\text{sol}}) / (f^2 l_B r_D d) \quad (9)$$

The magnitude of these polymer density oscillations causes the rate of change in the polymer surface coverage $\Delta \Gamma \approx \Delta \rho d$ (i.e., the increase of the polymer surface coverage per each deposition step) to be proportional to

$$\Delta \Gamma \approx (\epsilon_{\text{coh}} + \epsilon_{\text{sol}}) / (f^2 l_B r_D) \propto f^{-3/2} \quad (10)$$

where $r_D \approx (4\pi l_B f c)^{-1/2}$ is substituted for the Debye radius and c is the original monomer concentration in the solution. We can use this expression and estimate the ratio of this parameter for the partially and the fully charged systems, $\Delta \Gamma(0.5) / \Delta \Gamma(1) \propto 2^{3/2} \approx 2.8$. In our simulations, this value is close to 2.95 for systems comprised of short chains with degree of polymerization $N_p = 8$ (see Figure 9). We choose the system of the shortest chains for comparison since it is less susceptible to the finite size effects. This agreement is encouraging, however, to show that this theory is indeed capable of explaining the multilayer formation one has to consider the dependence of the polymer surface coverage rate on the cohesive energy and the Bjerrum length.

The model presented above can also be extended to include the effect of the counterion condensation which can be induced either by decreasing counterion size or by increasing the strength of the electrostatic interactions (increasing the value of the Bjerrum length, l_B). In this case, in addition to the electrostatic contribution to the layer formation, one has to take into account the counterion release effect as two oppositely charged chains intermix inside multilayers. This effect could be included by changing expression for the chains' bulk chemical potential and substituting the bare charge density, f , by the effective charge density, f^* , which should be found self-consistently by equating chemical potentials of free and condensed counterions. However, a detailed solution of this problem is beyond the scope of this paper and will be considered in a future publication.

Discussion and Conclusions

Our molecular dynamics simulations support the three-zone model describing the structure of a growing polymeric film. Zone 1 contains the layer in the vicinity of the surface which generally has one type of polyelectrolyte having a charge opposite to that of the surface (see Figures 3 and 6). The thickness of this zone is on the order of one molecular layer. Zone 2 contains complexes (symplexes) of polyelectrolytes of opposite charges. The layers in this zone are highly interpenetrated and essentially exhibit 1:1 charge stoichiometry. It should be noted that, despite the formation of such complexes, the alternating pattern

of charge excess is still preserved in the multilayers for all studied systems (see Figure 10). The dynamic exchange of polyelectrolytes between multilayers, then, occurs in such a way that the local density distribution is preserved. Zone 3 includes the outermost layer along with the counterions, the latter of which forms an electrical double layer. The overall multilayer charge neutrality is thereby maintained by these counterions. Interestingly, these counterions are excluded from the interior of the growing film, which is in agreement with experimental observations. This outermost polymeric layer evolves during the deposition of oppositely charged polyelectrolytes during the next step by forming complexes with the incoming polyelectrolyte chains.

It is well known that the local structure of the polyelectrolytes multilayers is similar to that of bulk polyelectrolyte complexes formed between oppositely charged macromolecules.^{39,40} This is also observed in our simulations where the conformations of the adsorbed chains inside layers are very similar to the structure of polyelectrolyte complexes in bulk solutions. We observed two different types of conformations, however, with regard to the different types of polyelectrolyte complexes. The complex structure between ionic groups on the charged surface and polyelectrolytes adsorbed during the first deposition step resembles that of a ladderlike complex.⁴¹ This is due to the fact that the surface charges are fixed and discrete and conformations of polyelectrolyte chains at the surface are close to rodlike ones that allow formation of well-organized ionic bonds in a ladderlike fashion between the charges on the surface and those on the polymer backbone. In contrast, the local structure of polyelectrolytes inside the multilayers and away from the surface is similar to a scrambled-egg complex⁴¹ structure where chains are more collapsed and intertwined. The transition between these two regimes occurs after the deposition of the first few layers (one to two steps in the case of our MD simulations). McAloney et al.⁴² have observed such transitions via AFM measurements of the first five layers where surface roughness increased with the number of deposited layers. We observe that the multilayers rearrange during the deposition process to form islands and holes that can better accommodate incoming chains. The formation of such islands and holes as seen in our simulations after the second deposition step (see Figures 2–4) is due to the conformational rearrangements of the polyelectrolytes during the deposition process. Because chains adsorbed during the first deposition step favor formation of a scrambled-egg complex, the resulting partial shrinkage of the chains exposes the surface and leaves uncovered spots, or holes. These holes are filled after two deposition steps by polyelectrolytes of similar charge, completing the formation of densely packed layers as seen in Figure 3b. Menchaca et al.⁴³ have observed the appearance of such polyelectrolyte–complex grains by liquid-cell AFM monitoring of the evolution of surface roughness during deposition of the first few layers.

Comparison of our simulation data with those obtained in the case of multilayer formation on charged spherical particles^{30,31} shows that the layers formed at charged surfaces show a higher degree of ordering. The reason for

(39) Farhat, T.; Yassin, G.; Dubas, S. T.; Schlenoff, J. B. *Langmuir* **1999**, *15*, 6621–6623.

(40) Yoo, D.; Shiratori, S. S.; Rubner, N. F. *Macromolecules* **1998**, *31*, 4309–4318.

(41) Michaels, A. S.; Miekka, G. J. *Phys. Chem.* **1961**, *65*, 1765.

(42) McAloney, R.; Sinyor, M.; Dudnik, V.; Cynthia, M. *Langmuir* **2001**, *17*, 6655–6663.

(43) Menchaca, J. L.; Jachimska, B.; Cuisinier, F.; Perez, E. *Colloids Surf., A* **2003**, *222*, 185–194.

this is the increase in available area around the spherical particle for adsorbing chains with each additional deposition step. Thus, the number of deposition cycles required for the completion of a single layer increases, giving rise to a high probability of mistakes in the layer structure. Even in the case of adsorption at a flat surface, considerable intermixing between chains deposited during subsequent steps still occurs. We note that such intermixing between layers has been neglected in previously proposed theoretical models of multilayer assembly.^{22,26} As we have already mentioned, several deposition steps are required to complete the formation of each layer. Nevertheless, the alternating pattern of surface charge excess is maintained for partially charged chains though the fluctuation amplitude is reduced due to chain interpenetration.

Short-range interactions play an important role in multilayer formation. We have performed simulations of the systems with $\epsilon_{LJ} = 0.25, 0.5, 0.75$, and $1.0 k_B T$. Only for $\epsilon_{LJ} = 0.75$ and $1.0 k_B T$ have we observed a steady film growth, while for $\epsilon_{LJ} = 0.25$ and $0.5 k_B T$, the layers stop growing after couple deposition steps. Similar behavior was observed even for a highly charged surface for which each surface particle was charged. It is important to point out that in our simulations we have used the same strength of the short-range interactions for polymer–polymer and polymer–surface pairs. The strong short-range interactions are necessary for polymer–surface interactions rather than for polymer–polymer ones. The strong polymer–surface interactions compensate for the electrostatic repulsions between similarly charged polymers, making formation of multilayers more favorable than complexation between oppositely charged polyelectrolytes in the bulk. This observation is in agreement with Kotov's results⁴⁴ which described the contribution of hydrophobic interactions between polyelectrolytes and the charged

surface, identifying them as the important factor determining the ability of the compounds to self-assemble via LbL assembly. Our simulation results are also in agreement with previous molecular simulations of layer formation near charged planar surfaces²⁸ and charged spherical particles,^{27,30,31} revealing the requirement of an extra short-ranged interaction in order to achieve successful polymeric film growth.

In conclusion, we have performed MD simulations of LbL deposition of polyelectrolytes from a dilute solution in order to study the effects of the fraction of charged monomer, as well as the chain degree of polymerization on the structure, stability, and mechanism of the multilayer formation. Polyelectrolyte chains in multilayers form scrambled-egg complexes of intertwined chains, thus increasing the amount of polymer adsorbed during each deposition step. For all of our simulations, approximately two deposition steps of similarly charged polymers were necessary to complete formation of a single compact layer. The polyelectrolyte chains are not perfectly stratified within the multilayered structure, but instead, there is intermixing between polyelectrolyte chains deposited during different depositions cycles. There are almost perfect periodic oscillations of density difference between positively and negatively charged chains after several deposition steps, despite the high degree of chain intermixing. Weakly charged chains allow significantly larger polymer encapsulation within layers than the strongly charged ones.

Acknowledgment. A.V.D. acknowledges funding from the National Science Foundation (DMR-0305203) and from the Petroleum Research Fund under the Grant No. PRF-39637-AC7.

(44) Kotov, N. A. *Nanostruct. Mater.* **1999**, *12*, 789–796.